第 35 卷第 10 期
2023 年 10 月

强 激 光 与 粒 子 束
HIGH POWER LASER AND PARTICLE BEAMS

Vol. 35，No. 10
Oct.，2023

·Ion Beam Science and Technology and Its Applications·

Radial probe detector system in the cyclotron of Heavy Ion Medical Machine*

Li Min[1,2]， Li Weilong[1]， Kang Xincai[1,3]， Chen Yucong[1]， Mao Ruishi[1,2]， Zhao Tiecheng[1]，
Feng Yongchun[1]， Zhou Kai[1]， Dong Jinmei[1]， Song Haihong[1]

（1. *Institute of Modern Physics*, *Chinese Academy of Sciences*, *Lanzhou* 730000, *China*;
2. *University of Chinese Academy of Sciences*, *Beijing* 100049, *China*;
3. *Lanzhou University of Technology*, *Lanzhou* 730050, *China*）

Abstract: The cyclotron is designed as the injector of the Heavy Ion Medical Machines (HIMMs) in Wuwei city and Lanzhou city, China. It provides 10 μA carbon ion beams to fulfill the accumulation requirement in the following synchrotron. Four picoammeters acquire the beam current signals gathered by the radial detectors; meanwhile, the beam time structure is measured with Field Programmable Gate Arrays and a real-time operating system. This paper introduces the mechanical design of the radial detectors and further provides the thermal structure analysis result of probe tips with and without water cooling. Moreover, the hardware and software architecture of the control system for this detector is described, including the motion control and data acquisition system, which can implement simultaneous acquisition of beam current data and position at more than 10 kS/s. At last, the laboratory test and acceptance scheme of both mechanical and control systems are listed, and the beam current and turn pattern measurement results at HIMMs are presented in this paper.

Key words: HIMM, cyclotron, radial detector, modularity, OPC UA

CLC number: TL56 **Document code:** A **doi**: 10.11884/HPLPB202335.220311

The first Heavy Ion Medical Machine (HIMMs) constructed by the Institute of Modern Physics, China[1-3] has passed the registration tests and entered clinical treatment in Wuwei city. A compact cyclotron is designed as the injector of a synchrotron which forms the HIMM, and it accelerates the $^{12}C^{5+}$ from the ion source to 7.0 MeV/u; meanwhile, the extracted beam current is more than 10 μA[4].

The radial probe detector plays an important role during the beam commissioning as well as the turn measurement, especially in monitoring the beam current varying under the condition of setting different physical parameters to estimate the machine characteristic and its acceptance[5-7]. As the compact structure of the cyclotron, two radial probes are installed on the hill and in the valley respectively. The one installed in the valley is used to monitor the beam current during the injection period, and the other one installed between the extraction deflector and extraction dipole is used to monitor the extraction beam current. Furthermore, the beam center measurement can be implemented with the two targets during the acceleration period. The radial probes installed in the cyclotron are shown in Fig.1.

1 Design of the radial probe system

The radial probe system is mainly composed of the physical and water-cooling optimization design, mechanical structure, interference shielding of weak signal measurement, data acquisition system, and motion control system.

1.1 Mechanical design

The radial probe target tips made up of one integral block and three differential fingers, which are distributed concurrently in the horizontal direction, can get the beam distribution in axial and radial directions by blocking the beam[8]. The three

* **Received date:** 2022-12-31； **Revised date:** 2023-08-23
Foundation item: National Natural Science Foundation of China (11905271; 12105336)
E-mail: Li Min, limin@impcas.ac.cn
Corresponding author: Kang Xincai, kangxincai@impcas.ac.cn

differential fingers are distributed uniformly in the vertical direction with a gap of 5 mm. The sizes of the integral and differential target tips are listed in Table 1. The three differential target tips protrude beyond the integral one by 0.5 mm to intercept the beam current for acquiring the beam distribution in the vertical direction. The radial probe target tips are made of copper. The top view of the radial probe is displayed in Fig.2, and the target probe structure of the radial probe is shown in Fig.3. Each radial probe is driven by a servo motor for closed-loop control of the position.

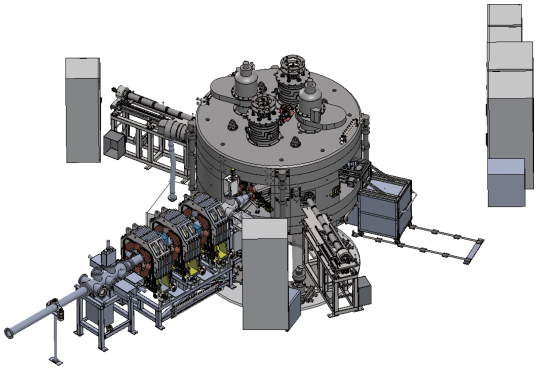

Fig. 1 Radial probes installed in the cyclotron of HIMM in Lanzhou

Table 1 Size of the integral and differential target tips

tip No.	tip name	size/mm
1	integral tip	40
2	differential tip−top	12
3	differential tip−middle	12
4	differential tip−bottom	12

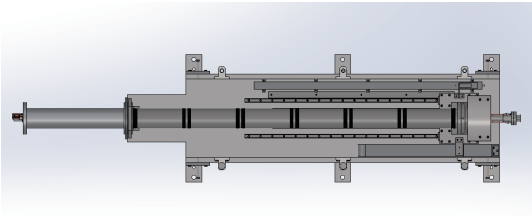

Fig. 2 Structure of the radial probe (top view)

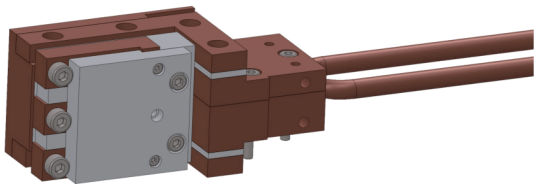

Fig. 3 Structure of the radial probes' tips

1.2 Thermal structural analysis

The extraction beam energy of the cyclotron is 7 MeV/u, and the beam current is 10 μA corresponding to the average power of 400 W. The Gaussian beam distribution with the size of 10 mm is used in the thermal structural analysis by COMSOL. The structures of the radial probe without and with water cooling are analyzed.

The target of the radial probe is made of oxygen-free copper. It can only achieve external heat transfer through the thermal radiation of the material surface to the environment without a water-cooling structure. From the simulation results shown in Fig.4, it can be seen that the temperature of the radial probes' target tips is more than 1400 ℃, which exceeds the melting point of the oxygen-free copper and can directly cause damage to the target. As a result, a water-cooled structure is a necessary design.

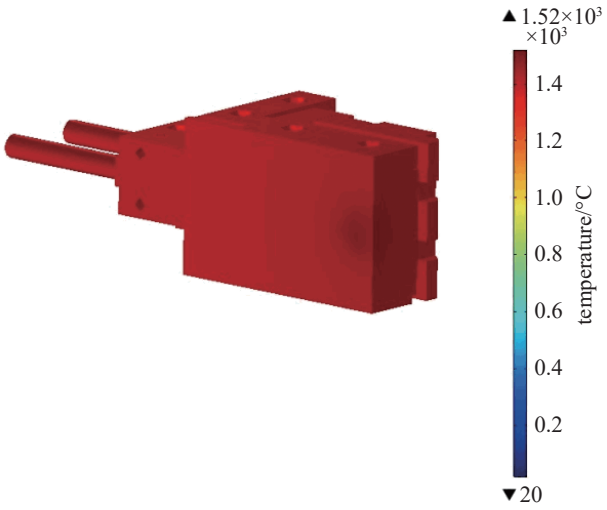

Fig. 4 Thermal structural analysis of the radial probe without water-cooling design

Because of the water-cooling structural design of the detector, where the support tube and the target are insulated by ceramics, the target transfers heat to the outside through the water pipe, then the heat convection conducts between the water pipe and the air in the water-cooling structure of the radial probe. While simulating the thermal characteristic of the water-cooling structure, the water-flow rate is set to 4 m/s, and the water pressure is set to 5 kg/cm^2. Meanwhile, the radiation heat transfer from a body (e.g., a black body) to its surroundings is proportional to the fourth power of the absolute temperature and can be expressed by equation (1)[9]

$$q = \varepsilon\sigma T^4 \quad (1)$$

where σ is a fundamental physical constant, T is the temperature, the emissivity ε is the effectiveness of a material's surface in emitting energy as thermal radiation and varies between 0.0 and 1.0. Here the emissivity coefficient of the oxygen-free copper is assumed as 0.1.

The result of the thermal analysis during the scanning process of the detector is shown in Fig.5. Fig.5 shows that the water-cooling structure gives a maximum surface temperature of less than 200 ℃, which is much lower than the melting point of oxygen-free copper of 1 083 ℃. Therefore, the water cooling structure with these designed parameters is in the range of thermal tolerance. What 's more, a layer of heat-conducting ceramic made of aluminum nitride is between the integral and the differential tips which can enhance the effect of water cooling[8].

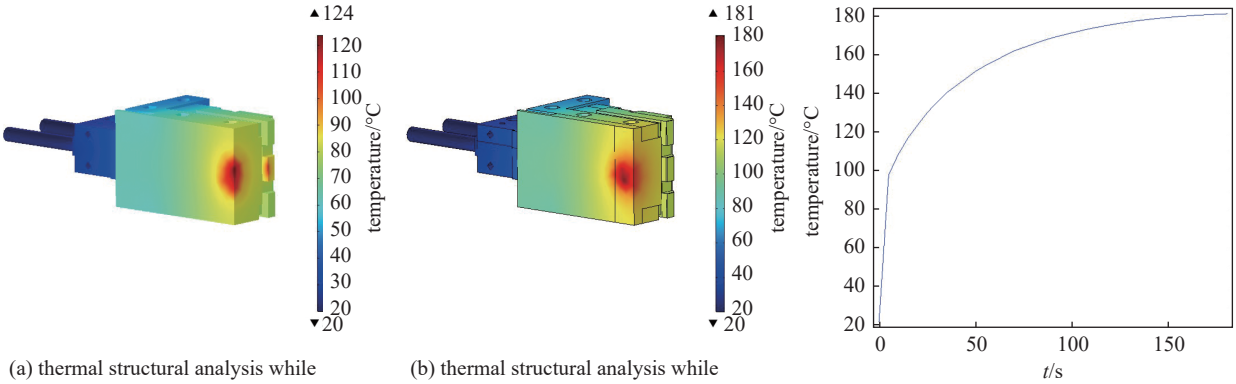

(a) thermal structural analysis while the differential target tips receive the highest beam power

(b) thermal structural analysis while the integral target tip receives the highest beam power

(c) temperature equilibrium curve while the integral target tip receives the highest beam power

Fig. 5 Thermal structural analysis of the radial probe with water-cooled design during the scanning process of the probe

During the scanning process with the probe from the outside towards the beam center of the cyclotron, in the first case, the differential target tips receive the highest beam power and reach the maximum temperature of 100 ℃ when the beam center is at the front edge of the detector, while the temperature of the integral target tip is 124 ℃ at this moment as shown in Fig.5(a).

Similarly, when the beam is completely intercepted by the integral target tip, the temperature of the entire detector is the highest that reaching 182 ℃, as shown in Fig.5(b). Meanwhile, the water temperature rises 3.2 ℃ when the maximum water flow velocity is 5 m/s. From the temperature equilibrium curve of the target, it can be seen that the temperature of the target tends to stabilize after about 3 min, as illustrated in Fig.5(c).

2 Control and data acquisition system

The radial probes are placed on the center plane of the magnetic pole gap of the cyclotron. It is mainly used to measure the radial and axial profiles of the beam and further get the information of radial and axial distribution of beam intensity inside the accelerator. The detectors are inserted from the central plane of symmetry in the valley or hill area of the cyclotron while measuring the beam information.

During the cyclotron commissioning period, it is required to localize the turns at the azimuth of the probes. The radius gains allow reconstructing the energy gain as a function of radius[6]. Simultaneously, the beam intensity signal from the radial probe tips is measured when it moves from the center to the extraction or vice versa. As a result, the control hardware of the radial probe is based on Field Programmable Gate Arrays (FPGAs), and a real-time (RT) operating system implements the requirements.

2.1 Hardware

The application of FPGA can realize precise timing, control, synchronization, and user-defined high-speed communication protocol requirements. The real-time operating system can ensure the realization of deterministic control, data processing and data logging[10-11]. Furthermore, the whole control system is based on the National Instrument(NI) CompactRIO hardware. The hardware architecture of this control and data acquisition system are shown in Fig.6.

The NI CompactRIO 9075[12] used in Wuwei city, which was upgraded to NI 9065[13] in Lanzhou city, is in charge of

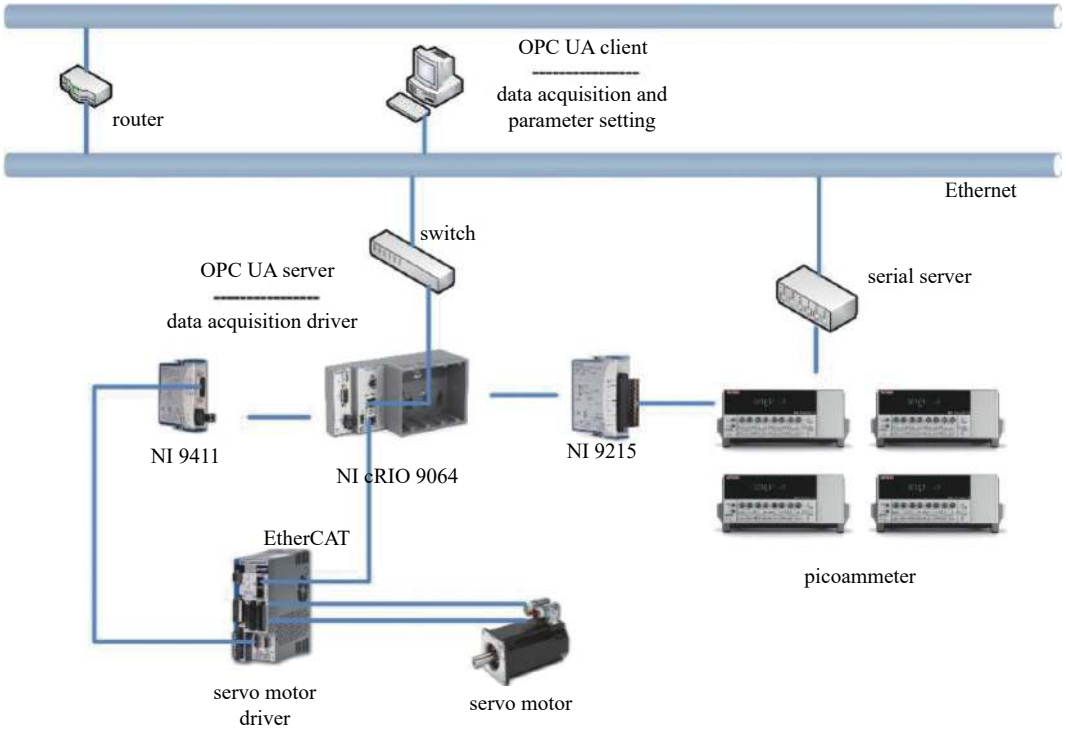

Fig. 6 Hardware framework of the radial probe control system

acquiring the beam current from the picoammeters where the beam current is converted to voltage linearly. In detail, the data acquisition and digital input/output functions were implemented on FPGA, where the raw analog data was first gathered by picoammeter and then further acquired by NI 9215 that performed 4-channel differential and simultaneous analog input (AI) at the maximum sample rate 100 kS·s^{-1}·ch^{-1} with 16-bit resolution[14]. The position information was input into the NI 9411[15] which worked with industrial logic levels and signals for direct connection to the motor driver whose resolution is 24 bits[16].

2.2 Software architecture

2.2.1 Software architecture

The software framework is designed and implemented with modularity technology organized by the producer-consumer design pattern (shown in Fig.7). The modularity design makes it fast to transplant the modules to the other similar projects of beam diagnostics front-end control system of the heavy ion accelerator transparently[17]. The automated variables publication of the OPC UA communication protocol[18] is implemented based on the XML configuration files shown in Fig.8[19]. Furthermore, it is validated the feasibility of accessing the database by OPC UA variables. The control information is sent into the beam diagnostics database developed with MariaDB[20]. Moreover, there are three tables designed for the target: the motion table, the DAQ table, and a static table consisting of the detector ’s installation, connection cables, and the network connection.

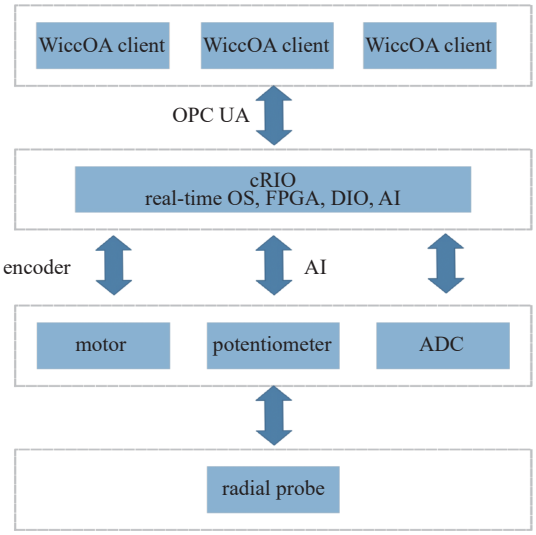

Fig. 7 Software framework of the radial probe control system

Based on the described hardware, the AI card can execute all channels of one radial probe detector simultaneously. Meanwhile, the position of the radial probe detector is read by the resolver, sampled simultaneously with the beam current signal at the FPGA and then transferred to RT by First In First Output (FIFO). Accordingly, the analog and digital data are finally parsed and converted into beam current and the position information at the GUI. Furthermore, the mechanical position precision is less than 1mm (nearly 0.5 mm) which means the whole control system can reach the 0.5 mm position precision

```
- <structure>
  - <folder name="BD">
    - <folder name="RD">
      - <folder name="20">
        - <folder name="01">
          - <folder name="cDAQ_setting">
              <item name="SamplePeriod" description="" initialValue="500" datatype="uint32" access="read/write"/>
              <item name="ReSampleNumber" description="" initialValue="0" datatype="uint32" access="read/write"/>
              <item name="Workingmode" description="" initialValue="0" datatype="boolean" access="read/write"/>
              <item name="Starttest" description="" initialValue="0" datatype="boolean" access="read/write"/>
              <item name="Stoptest" description="" initialValue="0" datatype="boolean" access="read/write"/>
              <item name="ErrorCode" description="" initialValue="True" datatype="uint32" access="read/write"/>
              <item name="Heartbeat" description="" initialValue="FALSE" datatype="int32" access="read/write"/>
              <item name="SaveData" description="" initialValue="FALSE" datatype="boolean" access="read/write"/>
            </folder>
          - <folder name="Motion">
              <item name="FindHome" description="" initialValue="FALSE" datatype="boolean" access="read/write"/>
              <item name="SetPosition" description="" initialValue="FALSE" datatype="double" access="read/write"/>
              <item name="Move" description="" initialValue="FALSE" datatype="boolean" access="read/write"/>
              <item name="StopMove" description="." initialValue="FALSE" datatype="boolean" access="read/write"/>
              <item name="PotentiometerPosition" description="." initialValue="0" datatype="double" access="read/write"/>
              <item name="EncoderPosition" description="." initialValue="0" datatype="double" access="read/write"/>
              <item name="FwdLimit" description="." initialValue="FALSE" datatype="boolean" access="read/write"/>
              <item name="RevLimit" description="" initialValue="FALSE" datatype="boolean" access="read/write"/>
              <item name="MotionState" description="." initialValue="FALSE" datatype="boolean" access="read/write"/>
              <item name="ResetEncoder" description="." initialValue="FALSE" datatype="boolean" access="read/write"/>
            </folder>
          - <folder name="Motionset">
              <item name="Startposition" description="." initialValue="0" datatype="double" access="read/write"/>
              <item name="Stopposition" description="." initialValue="0" datatype="double" access="read/write"/>
            </folder>
          - <folder name="RangeSet">
              <item name="Up" description="." initialValue="0" datatype="Int32" access="read/write"/>
              <item name="Middle" description="" initialValue="0" datatype="Int32" access="read/write"/>
              <item name="Down" description="." initialValue="0" datatype="Int32" access="read/write"/>
              <item name="Sum" description="." initialValue="0" datatype="Int32" access="read/write"/>
            </folder>
          - <folder name="DAQ">
              <item name="Up" description="" initialValue="0" datatype="Double" access="read/write"/>
              <item name="Middle" description="." initialValue="0" datatype="Double" access="read/write"/>
              <item name="Down" description="" initialValue="0" datatype="Double" access="read/write"/>
              <item name="Sum" description="." initialValue="0" datatype="Double" access="read/write"/>
            </folder>
          </folder>
        </folder>
      </folder>
    </folder>
  </structure>
```

Fig. 8 XML configuration file for radial probe control system

compared with the encoder position resolution.

The OPC UA server was developed and ran in the real-time operating system (VxWorks or Linux-RT); meanwhile the control logic was based on the state-machine design pattern executed at this terminal.

2.2.2 Main modules' introduction

The control system of this detector is mainly composed of three modules, which are described in the following.

(1) Parameters setting mainly includes three items: motor motion control parameters, front-end electronics control parameters, sampling mode and period, which can be set or controlled by these parameters.

(2) Real-time display and data storage mainly include beam current, position, and motion status information from the servo motor encoder readback. These data are further processed and indicated in different formats according to the requirement. During the measurement process, it is also necessary to save the beam current and the corresponding motor position in a file for offline processing and analysis.

(3) Motion control is used to control the system movement and monitor the motion status such as the limits, encoder position and potentiometer position, and so on.

2.3 Calibration and test in the laboratory

The offline assembly and test were implemented in the laboratory, including the mechanical and control systems.

2.3.1 Mechanical test

During the alignment and calibration of the radial probe, the laser tracker is used to calibrate the mechanical structure of the detector. The mounting flange of the detector is used as the benchmark; the flange circle is used as the zero point. The stability and moving distance were tested first. The moving distance of the radial probe is 796 mm, and the repeated positioning accuracy of the probe is less than 0.1 mm. The probe moves smoothly and the position fluctuation of the target during the movement process is less than ±0.5 mm. The insulation resistance between the probes and their outer casing is more than 1 000 MΩ, which can keep excellent insulation measured in the laboratory. The pressure resistance of the cooling system is 1.8 MPa, and the leakage rate of the detector's weld is less than 5.0×10^{-8} Pa·l·s^{-1}. All the above parameters were measured and

recorded before the on-site installation.

2.3.2 Test and calibration of data acquisition system

(1) Nonlinearity error verification

In the lab testing, the nonlinearity error verification of the front-end electronics of the radial probe is implemented with the current source, the CompactRIO control system, and the radial probe. Under the specified conditions, the maximum deviation for the calibration curve of the sensor is defined as the ratio between the fitted straight line (ΔY_{max}) and the percentage of the full-scale output (Y), which is called linearity (linearity is also called "non-linear error"). The smaller the value, the better the linearity characteristics. It is expressed as the following equation (2).

$$\delta = (\Delta Y\max / Y) * 100\% \quad (2)$$

Its verification flow is listed as follows:

① The noise voltage level of each channel of the CompactRIO system is measured without the output of the current source and saved as the noise file.

② The source outputs different current values fed into the front-end electronics. Then the output voltage of the front-end electronics is acquired with the CompactRIO control system by the NI 9215. Meanwhile, the data acquired more than 0.1 s by NI 9215 at the sample rate of 10 kS/s is averaged by using the developed average algorithms. The picoammeter has 8 ranges from 2 nA to 20 mA, while the beam current in the cyclotron is below 10 μA. As a result, the ranges below 20 μA are measured for the nonlinearity error test. The linear fitting between the set data and acquired data is plotted in Fig.9.

③ The data is subtracted by the noise and transformed into the current according to the transform coefficient.

④ The calculated data is then linearly fitted to analyze the nonlinearity error of each probe.

⑤ The control system will repeat the above flow until the nonlinearity error of the 5 ranges is measured.

According to the test results, the nonlinear error of 5 ranges for each probe is less than 1% after the data is linearly fitted.

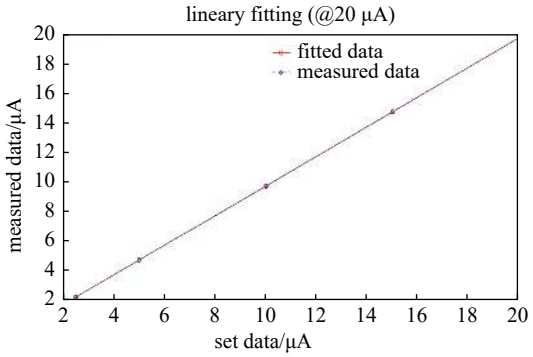

Fig. 9 Linear fitting between the set data and acquired data

(2) Resolution test of the control system

The resolution of the front-end electronics of the radial probe is also a required verification implemented according to the following procedures.

① Set the current source output to half of each front-end electronics range. For example, when the range is 10 μA, the set output of the current source is 5 μA, and then acquire the output value by NI 9215.

② Repeat the above measurement 100 times for each range, and save the measured data into a file.

③ Do statistics with the saved file and analyze the resolution error.

④ The control system will repeat the above flow until the resolution measurement of the four probes is finished.

The measured data is further counted with the parametric regression analysis method, assuming that the data distribution conforms to the Gaussian distribution. The statistical error for the resolution is less than 2% of the set range for each probe.

3 Experimental results

There are two radial probes installed in the cyclotron of HIMMs in Wuwei and Lanhzou city to monitor the beam current at different radial direction positions, tune measurement and turn pattern information, especially during the commissioning period of each machine. While measuring the beam turn pattern information, the start position, stop position, and motion parameters were pre-set. Then moving into the cyclotron center direction, the beam turns pattern and beam current accompanied by the position information were acquired and displayed in the GUI. Typically, the radial probe monitors the beam current at the target tips during the commissioning of the cyclotron. Fig.10 and Fig.11 are the monitoring results with the slow data acquisition system during cyclotron commissioning at the 3rd HIMM. The beam current measured is shown in Fig.10, which

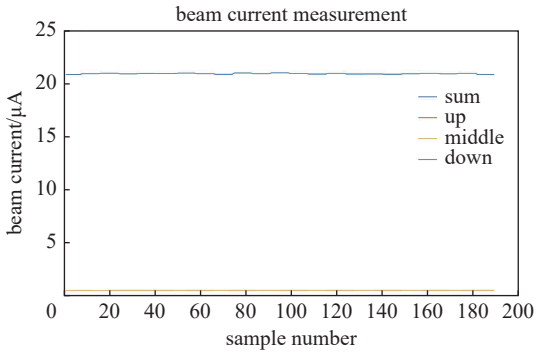

Fig. 10 Beam current measurement at a fixed position (150 mm from the cyclotron center)

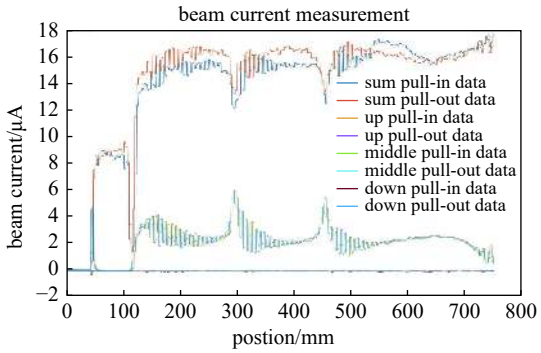

Fig. 11 Beam current measurement during the motion period (150 mm and 750 mm from the cyclotron center)

reaches more than 20.88 μA at a fixed position of 100 mm from the center of the cyclotron on the sum tip, and it is about 0.55 μA on the middle tip. In comparison, the value is 0.004 μA on both up and down tips close to the noise level. The beam current was continuously measured during uniform motion by pushing in the detector from 150 mm to 900 mm and then pulling it out in the opposite direction. The results shown in Fig.11 illustrate that the sum tip intercepted most of the beam particles. Likewise, the middle tip intercepted a small portion of the particles. The reverse limit of the detector is set as position 0. The distance from the reverse limit to the cyclotron center is 900 mm, however, the moving distance of the detector is 750 mm. As a result, the position 150 mm from the cyclotron center corresponds to 750 mm in the abscissa axis. Furthermore, the beam turn pattern was measured for machine performance study with the fast data acquisition system, Fig.12 shows the beam pattern test result of the valley radial probe with beam in Wuwei city in March 2021. All 4 probe tips' information is displayed and the sum information of the 4 channels is displayed simultaneously. Accelerator physicists can compare the data with that of the theoretical design and further study the machine performance.

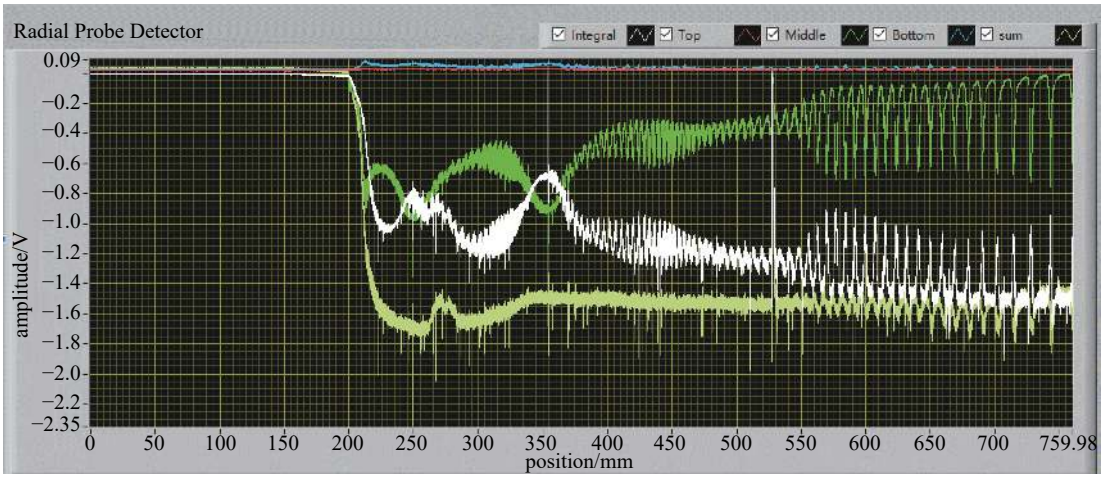

Fig. 12 Beam turns pattern measurement result

4 Conclusion

The radial probe is one of the essential devices for measuring the beam intensity in the cyclotron. It can further accurately calibrate other measuring devices because of its absolute measurement. Moreover, it also can be used as a low-energy beam stopper. To improve the system measurement accuracy, the probe's insulation resistance and shielding method were carefully designed and simulated on the water-cooling structure and thermal analysis to ensure the usage at high beam current. The data acquisition system is based on FPGA technology and a Keithley 6485 picoammeter, which has a high resolution of 20 fA. The mechanical structure and motion control was designed and developed based on the reliable scheme. The two radial probes installed in the HIMM cyclotron can measure the beam intensity at low energy region and get the beam turn pattern information. According to its application and the test results, the radial probe plays a vital role in the commissioning and operation period for HIMMs. As a result, it is essential to improve the efficiency of beam injection and extraction.

Acknowledgements The authors would like to thank the colleagues of the maintenance and operation team and beam diagnostics team from Lanzhou Ion Therapy Co., Ltd for their efforts in commissioning the target, and Li Peng, Zhang Jinquan, Wang Bing for their knowledge and instruction on the cyclotron.

References:

[1] Yang Jiancheng, Shi Jianchun, Chai Weiping, et al. Design of a compact structure cancer therapy synchrotron[J]. Nuclear Instruments and Methods in Physics Research Section A:Accelerators, Spectrometers, Detectors and Associated Equipment, 2014, 756: 19-22.

[2] Chai Weiping, Yang Jiancheng, Xia Jiawen, et al. Stripping accumulation and optimization of HIMM synchrotron[J]. Nuclear Instruments and Methods in Physics Research Section A:Accelerators, Spectrometers, Detectors and Associated Equipment, 2014, 763: 272-277.

[3] Shi Jian, Yang Jiancheng, Xia J W, et al. Heavy ion medical machine (HIMM) slow extraction commissioning[J]. Nuclear Instruments and Methods in Physics Research Section A:Accelerators, Spectrometers, Detectors and Associated Equipment, 2019, 918: 76-81.

[4] Hao Huanfeng. Design and development of a 7MeV/U heavy ion cyclotron[D]. Lanzhou: University of Chinese Academy of Sciences, 2014.

[5] Kleeven W. Some examples of recent progress of beam-dynamics studies for cyclotrons[C]//Proceedings of the 21st International Conference on Cyclotrons and Their Applications. 2016: 244-250.

[6] Baumgarten C. Beam based calibration measurements at the PSI cyclotron facility[C]//Proceedings of the 21st International Conference on Cyclotrons and Their Applications. 2016: 342-344.

[7] Sakamoto N, Fukunishi N, Kase M, et al. Acceleration of polarized deuteron beams with RIBF cyclotrons[C]//Proceedings of the 21st International Conference on Cyclotrons and Their Applications. 2016: 145-148.

[8] Guan Fengping, Xie Huaidong, Wen Lipeng, et al. The development of radial probe for CYCIAE-100[C]//Proceedings of the 20th International Conference on Cyclotrons and Their Applications. 2013: 165-167.

[9] Rao S S. Formulation and solution procedure[M]//Rao S S. The Finite Element Method in Engineering. 6th ed. Amsterdam: Elsevier, 2017: 505-522.

[10] NI. LabVIEW High-Performance FPGA Developer's Guide[EB/OL]. (2020-10-05). https://www.ni.com/zh-cn/support/documentation/supplemental/13/the-ni-labview-high-performance-fpga-developer-s-guide.html.

[11] NI. NI LabVIEW for CompactRIO developer's guide[EB/OL]. (2023-08-06). https://www.ni.com/pdf/products/us/fullcriodevguide.pdf.

[12] NI. cRIO-9075 and cRIO-9076 user manual and specifications[EB/OL]. (2023-06-27). https://www.ni.com/docs/zh-CN/bundle/crio-9075-9076-seri/resource/375650d.pdf.

[13] NI. cRIO-9065 specifications[EB/OL]. (2023-08-14). https://www.ni.com/docs/zh-CN/bundle/crio-9065-specs/page/specs.html.

[14] NI. NI-9215 specifications[EB/OL]. (2023-08-14). https://www.ni.com/docs/zh-CN/bundle/ni-9215-specs/page/specs.html.

[15] NI. NI-9411 specifications[EB/OL]. (2023-07-20). https://www.ni.com/docs/zh-CN/bundle/ni-9411-specs/page/specs.html.

[16] AKM synchronous servomotors[EB/OL]. (2022-04-28). https://www.kollmorgen.cn/sites/default/files/akm/documentation/installation//AKM%20Installation%20Manual%20EN%20Rev%2006-2008.pdf.

[17] Li Min. The design and implementation of front-end control system of beam diagnostics for HIMM[D]. Lanzhou: Institute of Modern Physics, University of Chinese Academy of Sciences, 2015.

[18] Huang Rui. Research on key technology of PLC programming environment development supporting client-edge-cloud collaboration[D]. Wuhan: Huazhong University of Science and Technology, 2022.

[19] Wu Jianxin. Design and implementation of satellite telemetry data processing system based on XML technology[D]. Xi'an: Xidian University, 2019.

[20] Huang Zhixin. Design and implementation of an information collection subsystem for operator cloud[D]. Beijing: Beijing University of Posts and Telecommunications, 2020.

医用重离子回旋加速器径向探针系统

李 敏[1,2], 李维龙[1], 康新才[1,3], 陈玉聪[1], 毛瑞士[1,2], 赵铁成[1],
冯永春[1], 周 凯[1], 董金梅[1], 宋海宏[1]

(1. 中国科学院 近代物理研究所, 兰州 730000; 2. 中国科学院大学, 北京 100049; 3. 兰州理工大学, 兰州 730050)

摘 要: 武威和兰州重离子加速器使用回旋加速器作为其注入器。回旋加速器为该装置的同步加速器提供 10 μA 的碳离子束流以满足其物理需求。而径向探针则是安装在回旋加速器内部实现束流流强和圈图测量的重要束诊元件。径向靶头上的束流信息经前端电子学拾取后会进一步进入数据采集系统,最终实现回旋加速器的束流流强和圈图测试。其中,径向探针的前端电子学采用皮安表,数据采集系统基于实时操作系统和 FPGA 技术。介绍了径向探针的机械结构设计,并分析了探头有无水冷结构的热结构;描述了控制系统软硬件架构,可以实现 10 kHz 的数据和位置信息的同步采集。最后,还介绍了探针机械和控制系统的实验室测试和验收标准以及在束测量结果。

关 键 词: HIMM; 回旋加速器; 径向探针; 模块化; OPC UA